Experimental measurement of the wake field in a plasma filament created by a single-color ultrafast laser pulse

Yan Peng,[1] Bowei Xu,[1] Shiwei Zhou,[1] Zhaozhao Sun,[1] Haicheng Xiao,[1] Jiayu Zhao,[1] Yiming Zhu,[1,*] Xi-Cheng Zhang,[2] Daniel M. Mittleman,[3] and Songlin Zhuang[1]

[1]*Terahertz Technology Innovation Research Institute, Terahertz Spectrum and Imaging Technology Cooperative Innovation Center, Shanghai Key Lab of Modern Optical System, University of Shanghai for Science and Technology, Shanghai 200093, People's Republic of China*

[2]*The Institute of Optics, University of Rochester, Rochester, New York 14627, USA*

[3]*School of Engineering, Brown University, Providence, Rhode Island 02912, USA*

(Received 30 March 2020; revised 11 November 2020; accepted 2 December 2020; published 23 December 2020)

A laser plasma wake field in a single-color femtosecond laser filament determines the acceleration of ionized electrons, which affects the intensity and bandwidth of the emitted terahertz wave and is important for understanding the fundamental nonlinear process of THz generation. Since the THz wave generated by a laser wake field is extremely small and easily hidden by other THz generation mechanisms, no method exists to measure this wake field directly. In this paper, a simple and stable method for determining the amplitude of the laser plasma wake field is presented. Based on the cancellation of a positive laser plasma wake field and an external negative electric field, the "zero point" of the intensity of the generated THz wave at some frequency can be used to determine the exact amplitude of the corresponding laser plasma wake field. This finding opens an avenue toward the clarification of ultrafast electronic dynamic processes in laser-induced plasmas.

DOI: 10.1103/PhysRevE.102.063211

I. INTRODUCTION

In recent years, terahertz (THz) waves have been widely applied in many fields of research, including electronics [1–3], life science [4,5], and spectroscopy [6–11]. Several methods have been used to generate THz waves, such as photoconductive antennas [8–10], optical rectification [11–14], electron accelerators [15–17], and laser filaments [18–21]. In particular, the laser filament method can generate an ultrabroadband spectrum of THz radiation [20,21]. Specifically, by focusing the radially polarized THz beam generated from a single-color laser pulse-induced filament, one can obtain a longitudinal field component, which can be used for the investigation of super-resolution microscopy and optical storage [22,23].

For a single-color laser filament, the THz electromagnetic emission is produced by the longitudinal oscillations of the plasma left in the wake of the moving ionization front. The corresponding laser plasma wake field determines the acceleration of ionized electrons and thus has a direct impact on the intensity and bandwidth of the emitted THz wave, which is important for understanding the fundamental nonlinear process of THz generation. However, because the THz wave generated by the laser wake field is extremely small and easily hidden by other THz generation mechanisms (the THz energy in the single-color laser case is one thousandth less than that of the two-color laser case), direct measurement of the amplitude of the laser plasma wake field has not been possible.

In this paper, we present a method for the experimental determination of the laser plasma wake field [24,25]. The method is based on the cancellation of the local field resulting from a positive laser plasma wake field and an externally applied negative electric field. Here, the single-color laser filament is chosen as the THz producing method, in which the laser wake field is the only physical origin of THz generation. Specifically, the key point of this method is the implementation of an external direct current (DC) electric field, which is superposed with the laser-induced wake field. Depending on the electron acceleration driven by the net electric field in the plasma, the intensity of the generated THz wave could be varied. When the net electric field reaches its zero point, the electrons experience zero acceleration, and no THz wave is formed. Therefore, the exact value of the laser plasma wake field can be directly obtained from that of the external electric field.

II. SIMULATION

Several theories related to THz generation exist, including parametric decay theory [26] and electric quadrupole theory [27], which mainly focus on the on-axis propagation of the terahertz wave, and the transition-Cherenkov model [18,24,25], which focuses on the mechanism of THz emission by analyzing the electron current spectrum. Considering that the main goal of our research is the electron current spectrum of the laser plasma wake field, we use the transition-Cherenkov model as our theoretical basis. This is discussed in more detail in the following.

When a high-intensity laser pulse ionizes a gas, a laser plasma is formed with a plasma frequency of $\omega_{pe} = \sqrt{e^2 n_e / m_e \varepsilon_0}$, which directly depends on the ionized electronic density n_e [24,25]. The lifetime of this laser plasma is

*Corresponding author: ymzhu@usst.edu.cn

approximately 1 ns [24,25]. As the laser pulse propagates forward, an electric dipole is generated and moves at the group velocity of light along the propagation axis. This moving dipole generates electromagnetic emission in the THz range [28–31]. Based on the transition-Cherenkov model, the spectral energy density of the THz radiation can be written as [18,24,25]

$$\frac{d^2W}{d\omega d\Omega} = \frac{\left|j_z^w(\omega)\right|^2}{4\pi\varepsilon_0 c}\frac{\rho_0^4\sin^2\theta}{(1-\cos\theta)^2}\sin^2\left(\frac{L\omega}{2c}(1-\cos\theta)\right), \quad (1)$$

where W is the spectral energy of THz radiation, $j_z^w(\omega)$ is the Fourier spectrum of the electron current, ε_0 is the permittivity of vacuum, c is the free-space light speed, $\rho_0 = 250\,\mu$m is the diameter of the filament, θ is the radiation angle of the THz wave with a frequency of ω, and $L = 10$ mm is the length of the filament. For a laser pulse of duration $\tau_L = 30$ fs and a maximum intensity $I_0 = 1\times10^4\,\mathrm{W/cm^2}$, with a $\sin^2$ temporal shape, $I(t) = I_0\sin^2(\pi t/\tau_L)$. Deduced from the wave equation [18,31], the equation for the current spectrum $\vec{\mathbf{j}}_z^{\,w}$, THz frequency ω, and plasma wake field E_L can be obtained as follows:

$$\vec{\mathbf{j}}_z^{\,w} = \varepsilon_0\omega_{pe}\vec{\mathbf{E}}_L\frac{\omega+2iv_e}{\omega_{pe}^2-\omega^2+iv_e\omega}\frac{\sin(\omega\tau_L/2)}{1-(\omega\tau_L/2\pi)}\exp\left(-\frac{i\omega\tau_L}{2}\right), \quad (2)$$

where $\vec{\mathbf{E}}_\mathrm{L}$ is the laser plasma wake field originating from the laser pondermotive force and its amplitude A_L can be expressed as $A_L = e\omega_{pe}I_0/2m_e\varepsilon_0c^2\omega_0^2$. The parameter m_e is the mass of the electron, $v_e = 1$ THz is the electron collision frequency, and ω_{pe} is above 1.7 THz with $n_e = 1\times10^{21}\,\mathrm{m^{-3}}$.

When a longitudinal external electric field $\vec{\mathbf{E}}_\mathrm{e}$ is applied to the filament, it produces a new additional electron current. This externally induced current can be written as

$$\vec{\mathbf{j}}_z^{\,e} = \frac{\varepsilon_0\omega_{pe}^2\vec{\mathbf{E}}_e}{\omega^2-\omega_{pe}^2+iv_e\omega}. \quad (3)$$

According to Eq. (3), the definition of $\vec{\mathbf{j}}_\mathrm{z}^{\,\mathrm{e}}$ is related to n_e and $\vec{\mathbf{E}}_\mathrm{e}$. We note that once the electron density n_e is zero, the current $\vec{\mathbf{j}}_\mathrm{z}^{\,\mathrm{e}}$ will be zero, regardless of the value of the external electric field $\vec{\mathbf{E}}_\mathrm{e}$. For the external electric field $\vec{\mathbf{E}}_\mathrm{e}$, The voltage may be limited to remain below the value that would generate a spark or plasma in the gas medium. In this case, the current driven by this external electric field can last only to the end of the lifetime of the plasma generated by the initial laser pulse, which is approximately 1 ns. Until the arrival of the next pump laser pulse, the external DC field generates no current. Inspired by these considerations, we perform the following theoretical analysis and experiments.

When the internal laser wake field and external electric field exist at the same time, the total electron current spectrum is a vector sum of Eqs. (2) and (3), which can be written as $\vec{\mathbf{j}}_\mathrm{z}^{\,\mathrm{w+e}} = \vec{\mathbf{j}}_\mathrm{z}^{\,\mathrm{w}} + \vec{\mathbf{j}}_\mathrm{z}^{\,\mathrm{e}}$. If $\vec{\mathbf{E}}_\mathrm{L}$ and $\vec{\mathbf{E}}_\mathrm{e}$ have the same direction, then the current amplitudes follow $j_z^{w+e}(\omega) = j_z^w(\omega) + j_z^e(\omega)$; if $\vec{\mathbf{E}}_\mathrm{L}$ and $\vec{\mathbf{E}}_\mathrm{e}$ have different directions, then the current amplitudes follow $j_z^{w-e}(\omega) = j_z^w(\omega) - j_z^e(\omega)$. The computed values for the amplitudes of the current spectrum originating from the laser plasma wake field $j_z^w(\omega)$, the external electric field $j_z^e(\omega)$, and the total current spectrum $j_z^{w+e}(\omega)$ as a function of the THz frequency are shown in Fig. 1.

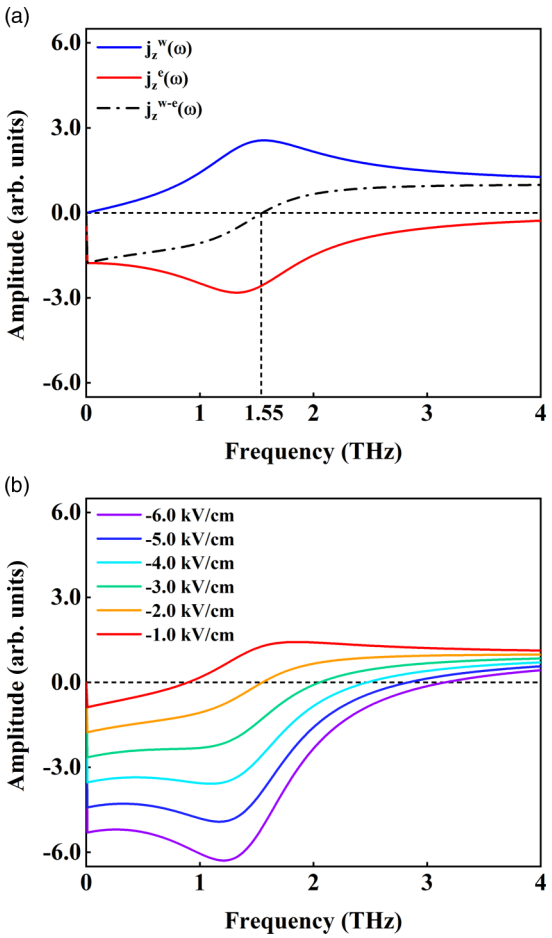

FIG. 1. (a) Simulation result of the amplitude of the current spectrum originating from the laser plasma wake field [$j_z^w(\omega)$, blue (upper) solid line], the external electric field [$j_z^e(\omega)$, red (lower) solid line], and the sum of the two [$j_z^{w+e}(\omega)$, black dot dash line] for an external electric field of -2 kV/cm. (b) The amplitude of the total current spectrum for different values of the external electric field.

In these plots, the positive and negative values represent the direction of the field, with the positive direction defined as the direction of the propagation of the laser pulse. Taking the case of adding a -2 kV/cm external electric field as an example [see Fig. 1(a)], the amplitude of $j_z^w(\omega)$ increases rapidly and then decreases slowly, while the amplitude of $j_z^e(\omega)$ increases slowly and then decreases rapidly. Because the two fields have opposite directions, the net current spectrum crosses through zero at a frequency of 1.55 THz [the black dash-dotted line in Fig. 1(a)]. Additionally, for the different values of the external electric field, the amplitude of $j_z^{w-e}(\omega)$ changes such that this zero crossing appears at different THz frequencies, as illustrated in Fig. 1(b). Therefore, based on the values of the THz frequency at which zero crossing occurs and the known value of the external electric field, the unknown laser plasma wake field can be extracted.

We also note that the plasma wake field originates from the oscillating laser field, leading to a value of the wake field that varies in time and space. As the amplitude of the wake field increases, both the amplitude and spectral width of the generated THz signal also increase. Therefore, the fixed frequency component corresponds to a fixed value of the wake field.

A robust procedure for extracting the value of this wake field is as follows. We can compute the amplitude of each spectral component of the broadband THz wave generated by this ultrafast current. Clearly, as implied by Fig. 1, THz components with different frequencies should have different variations with the applied DC field. From this variation, the amplitude of the laser plasma wake field inside the filament can be determined. The relation among the THz energy, THz frequency, laser plasma wake field, and external electric field can be written as

$$\frac{d^2W}{d\omega d\Omega} = \frac{\left|j_z^w(\omega) + j_z^e(\omega)\right|^2}{4\pi\varepsilon_0 c} \frac{\rho_0^4 \sin^2\theta}{(1-\cos\theta)^2} \times \sin^2\left(\frac{L\omega}{2c}(1-\cos\theta)\right). \quad (4)$$

The physical mechanism can be understood from the process of electron motion. Specifically, when an external electric field is added along the laser filament direction, the electrons liberated by the laser field around the peak of the femtosecond pulse are accelerated by the synthesized longitudinal electric field originating from the superposition of the laser plasma wake field and the external electric field. The wake field originating from the laser ponderomotive force is directed along the direction of the laser propagation (defined as positive, as noted above). When the external electric field is added along the filament in the same direction, the positive external voltage can increase the amplitude of the net electric field and thus enhance the strength of the generated THz wave.

The higher the positive external voltages are, the stronger the electron acceleration is, and the higher the THz radiation intensity is. In the opposite case of a negative external voltage, the intensity of the net electric field decreases first, until it reaches zero, and then increases in the opposing direction as the external negative electric field gradually exceeds the positive laser plasma wake field in magnitude. The corresponding electron acceleration also experiences the process of weakening in the beginning, the zero point, and then strengthening in the opposite direction.

The simulated results are shown in Fig. 2(a), with several particular frequency components (0.5, 1.5, 2.0, and 2.5 THz) taken as examples. We see that for each component of the THz emission, the THz field amplitude varies quadratically with the applied DC field, as implied by Eq. (4). Moreover, for each frequency, there is a zero point corresponding to no THz generation, and the value of the applied DC field that induces this zero point shifts toward a higher negative voltage as the THz frequency increases.

For the zero point of one frequency component, its THz amplitude is zero; i.e., $j_z^{w-e}(\omega) = j_z^w(\omega) - j_z^e(\omega) = 0$. Combining the E_e value in Fig. 2(a) and Eqs. (2) and (3), we can obtain the corresponding wake field of E_L [Fig. 2(b)]. For example, if the zero point is emitted at 1.5 THz, the corresponding plasma wake field is 3.3×10^4 V/cm [Fig. 2(b)].

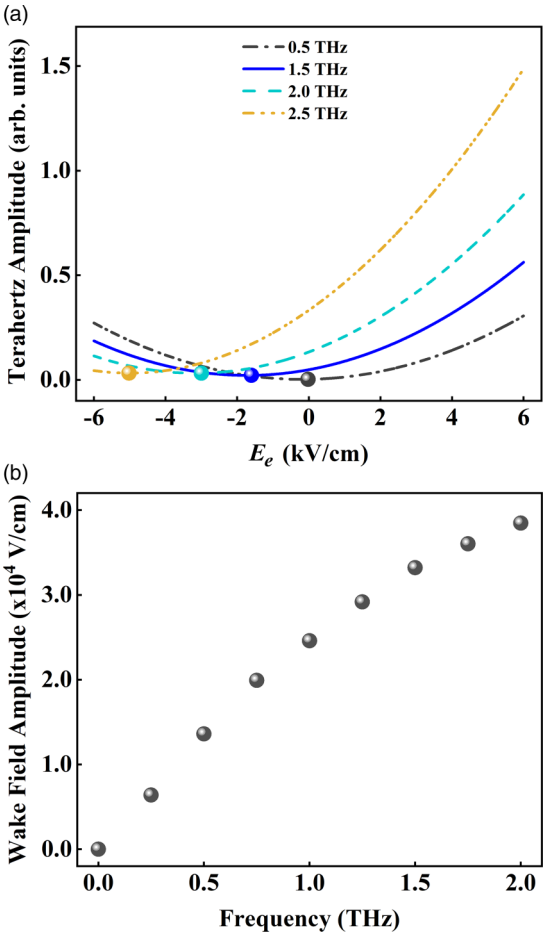

FIG. 2. Theoretical relations among the THz frequency, the external electric field, and the amplitude of the laser plasma wake field. (a) Simulation result of THz radiation at different frequencies as a function of the external electric field. The black (dot dash), blue (solid), green (dash), and orange (double-dot dash) lines represent THz frequencies of 0.5, 1.5, 2.0, and 2.5 THz, respectively. (b) The calculated amplitude of the laser plasma wake field E_L as a function of the generated THz frequency.

III. EXPERIMENT RESULTS

To support this theoretical analysis, we performed experiments using the setup shown in Fig. 3.

We used a commercial laser amplifier system with a repetition rate of 1 kHz, a pulse duration of 130 fs, a central wavelength of 800 nm, and an average laser pulse energy of 8 mJ. The output laser beam was divided into two beams (1:9 ratio) at beam splitter L1. The weaker beam was used as the probe beam for electro-optic (EO) sampling, and the stronger beam was focused in a dry air medium (humidity ~3%) to form a filament that then generates the radially polarized THz wave. This radial THz beam was focused by a parabolic mirror (5 cm diameter) and detected with the EO technique. We used a 200-μm-thick ⟨100⟩ cut ZnTe crystal for the detection of the longitudinal electric field

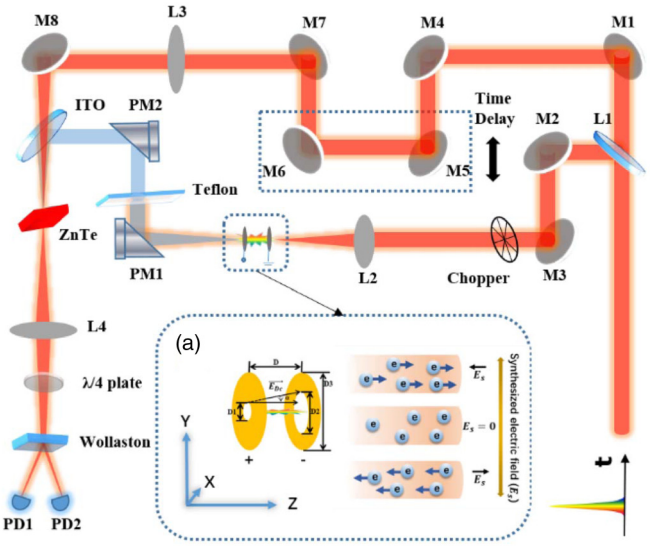

FIG. 3. Schematic diagram of the experimental setup showing the generation and detection of THz radiation. The orientation of the EO crystal and optical detection polarization are chosen to measure the appropriate THz field polarization. Inset (a) shows the construction of two circular copper electrodes and the direction of electron movement in the laser plasma under the synthesized electric field.

component [18,24]. A static external electric field was added along the filament by two circular copper electrodes, as shown in Fig. 3(a). The distance between the two electrodes was 12 mm, slightly larger than the length of the laser filament (10 mm). The diameter of the hole in the first electrode was 3 mm, while the diameter of the hole in the second electrode was 20 mm (to avoid the effect of the electrode on the outgoing THz radiation), corresponding to an electric field angle of nearly 35.0 °.

To remain below the threshold of spontaneous sparking discharge, the DC voltage was varied from −6 kV to +6 kV with a step of 0.5 kV, which corresponds to a field of approximately −4.0 kV/cm ∼+4.0 kV/cm with a step of 0.3333 kV/cm.

The experimental results and their quadratic fit curves are summarized in Fig. 4.

The formula of the quadratic fit curves for 0.1, 0.5, 1.0, and 1.5 THz is as follows:

$$W_{0.1\mathrm{THz}}(E_e) = 0.009\,85E_e^2 + 0.012\,09E_e + 0.094\,68, \quad (5)$$

$$W_{0.5\mathrm{THz}}(E_e) = 0.021\,09E_e^2 + 0.046\,92E_e + 0.271\,12, \quad (6)$$

$$W_{1.0\mathrm{THz}}(E_e) = 0.020\,92E_e^2 + 0.095\,17E_e + 0.415\,06, \quad (7)$$

$$W_{1.5\mathrm{THz}}(E_e) = 0.018\,22E_e^2 + 0.128\,81E_e + 0.507\,42. \quad (8)$$

We clearly see that for each spectral component of the THz emission, the intensity indeed varies quadratically with the electric field, as predicted. The zero point shifts toward a higher negative voltage with increasing THz frequency. From these data, we find, for example, for the generated THz frequency of 1.5 THz, the value of the external field that

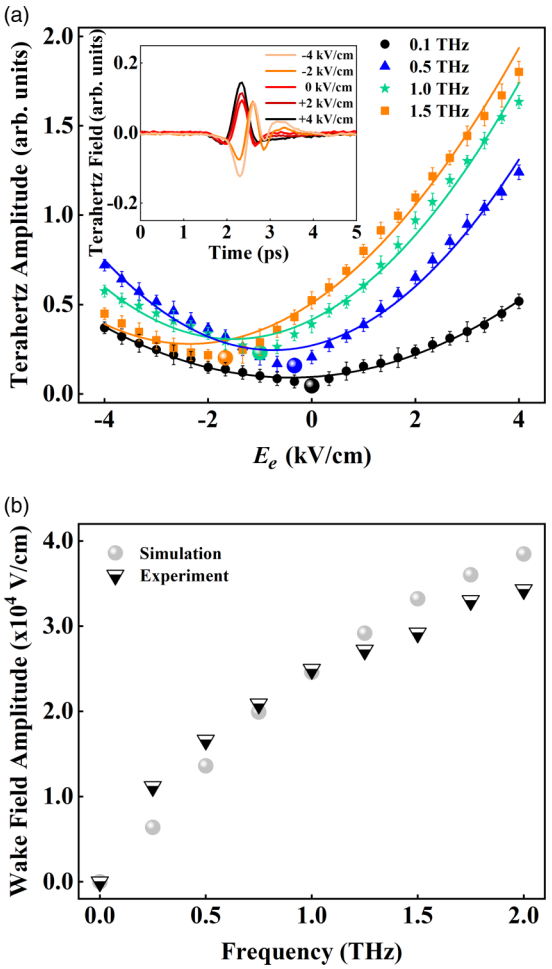

FIG. 4. Experimental measured relations among the THz frequency, external electric field and amplitude of the laser plasma wake field. (a) Measured THz radiation with different frequencies under different external electric fields and their quadratic fit curves. The black (circle), blue (triangle), green (star), and orange (square) points represent a THz frequency of 0.1, 0.5, 1.0, and 1.5 THz, respectively. The inset shows several examples of the measured time-domain electric fields. (b) Comparison of the amplitude of the laser plasma wake field E_L corresponding to different THz frequencies (black triangles) with the calculated results (gray circles).

produces the minimum THz field amplitude is approximately −1.7 kV/cm. With this value, the corresponding amplitude of the laser plasma wake field can be obtained from Eqs. (2) and (3) as 3.0×10^4 V/cm, which is slightly smaller than the calculated results. This small difference occurs because the effective detection bandwidth of the ZnTe crystal is centered at 1.0 THz and decreases on both sides [32]. Additionally, in Fig. 4(a), we observe that the measured zero points are not strictly zero values for the generated field component. This value may be because the experimental voltage setting cannot be tuned to precisely the same value as that of the laser plasma wake field. The small difference induces a nonzero value of the THz energy. Another possible reason for this phenomenon is that the laser wake field value is not uniform throughout the entire length of the filament, so canceling it at one point is possible, but canceling it everywhere is not

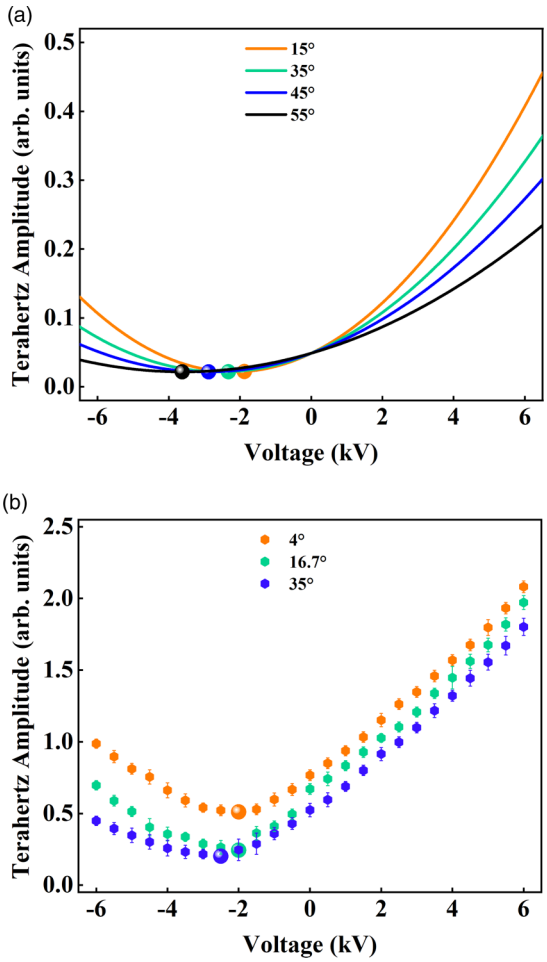

FIG. 5. The dependence of the zero point position of the 1.5-THz component on the angle of the external electric field. (a) The solid line from upper to lower are simulated intensity evolution of the THz amplitude as a function of the external electric field with an angle of 15 °, 35 °, 45 °, and 55 °, respectively. (b) The dot line from upper to lower are measured intensity evolution of the THz amplitude as a function of the external electric field with an angle of 4 °, 16.7 °, and 35 °, respectively.

possible. Nevertheless, a clear minimum in the generated THz magnitude must correspond to the minimum in the induced current, so the above analysis is still valid for estimating the magnitude of the laser wake field.

An additional factor that should be considered relates to the fact that the internal diameters of the two circular copper electrodes along the filament are different. It is therefore clear that the direction of the externally generated electric field must change along the filament. This change will affect the enhancement of THz wave components with different frequencies. To evaluate this effect, we also theoretically and experimentally investigated the effect of the external electric field direction on the observed zero points.

For Eqs. (3) and (4), $\vec{\mathbf{E}}_e = V/L\cos\alpha$, where $\alpha = \arctan(\Delta d/2D)$ is the direction of the external electric field. Taking the 1.5-THz component as an example, the simulation results are as shown in Fig. 5(a).

We see that as the angle between the external electric field and the propagation axis increases, the intensity of the generated THz wave drops quickly, and the zero point shifts toward a higher opposite voltage. We conclude that as the angle α increases, the voltage V needs to be increased to obtain the same effective value of the external electric field E_e. We can confirm the validity of this analysis by performing additional experiments, where we vary the diameter of the aperture in the second electrode to change the field angle. In the experiments, the diameters of the holes in the second electrode were 5, 10, and 20 mm, corresponding to electric field angles of 4.0°, 16.7°, and 35.0°, respectively. As presented in Fig. 5(b), the measured shift of the minimum or zero point for the 1.5-THz field component is consistent with the simulation results in Fig. 5(a).

Notably, there exists some difference between the theoretical calculation and the experimental results. We believe there are two reasons: (1) In the simulation calculation, the change step of the external electric field can be small and accurate, which is 0.01 kV/cm. Therefore, the zero point of the different frequency THz wave energies can be accurately found. In the experiment, the change step of the external voltage is 0.5 kV, which, combined with the external voltage angle, gives the distance between the two electrodes ($\vec{\mathbf{E}}_e = V/L\cos\alpha$), and the change step of the external electric field along the filament direction is 0.3333 kV/cm. Therefore, there is a certain deviation between the experimental results and the calculated values in terms of the intensity of the external electric field and the corresponding wake field amplitude. (2) There is an unavoidable error caused by the jitters in the laser device and other mechanical devices, measurement errors, and instrument precision.

IV. CONCLUSION

In conclusion, we exploit the ultrafast generation and picosecond lifetime of a laser-induced plasma to control the magnitude and direction of the net electric field experienced by liberated electrons. By measuring the generated THz wave, we demonstrate a unique method for the quantitative determination of the magnitude of the laser plasma wake field. Depending on the zero point position of the magnitude of the THz wave with the specific frequency, the corresponding amplitude of the laser plasma wake field can be determined. These results will be important for optimizing the THz generation process as well as clarifying the physics of ultrafast charge dynamics in a laser-induced plasma [4,7,33–36].

ACKNOWLEDGMENTS

National Natural Science Foundation of China (Grants No. 61771314, No. 61922059, and No. 81873609); the 111 Project (D18014); the International Joint Lab Program supported by Science and Technology Commission Shanghai Municipality (Grant No. 17590750300); the Key project supported by Science and Technology Commission Shanghai Municipality (Grant No. YDZX2019310-0004960).

[1] M. Tonouchi, Nat. Photonics **1**, 97 (2007).

[2] Y. Shin, L. R. Barnett, D. Gamzina, N. C. Luhmann Jr, M. Field, and R. Borwick, Appl. Phys. Lett. **95**, 181505 (2009).

[3] O. Schubert, M. Hohenleutner, F. Langer, B. Urbanek, C. Lange, U. Huttner, D. Golde, T. Meier, M. Kira, S. W. Koch, and R. Huber, Nat. Photonics **8**, 119 (2014).

[4] W. Chen, Y. Peng, X. Jiang, J. Zhao, H. Zhao, and Y. Zhu, Sci. Rep. **7**, 12166 (2017).

[5] A. Markelz, S. Whitmire, J. Hillebrecht, and R. Birge, Phys. Med. Biol. **47**, 3797 (2002).

[6] W. P. Leemans, C. G. R. Geddes, J. Faure, Cs. Tóth, J. van Tilborg, C. B. Schroeder, E. Esarey, G. Fubiani, D. Auerbach, B. Marcelis, M. A. Carnahan, R. A. Kaindl, J. Byrd, and M. C. Martin, Phys. Rev. Lett. **91**, 074802 (2003).

[7] Y. Peng, X. Yuan, X. Zou, W. Chen, H. Huang, H. Zhao, B. Song, L. Chen, and Y. Zhu, Biomed Opt Express. **7**, 4472 (2016).

[8] R. M. Arkhipov, A. V. Pakhomov, M. V. Arkhipov, A. Demircan, U. Morgner, N. N. Rosanov, and I. Babushkin, Phys. Rev. A **101**, 043838 (2020).

[9] I. C. Benea-Chelmus, C. Bonzon, C. Maissen, G. Scalari, M. Beck, and J. Faist, Phys. Rev. A **93**, 043812 (2016).

[10] C. Z. Wu, S. Khanal, J. L. Reno, and S. Kumar, Optica. **3**, 734 (2016).

[11] J. Y. Zhao, W. Chu, Z. Wang, Y. Peng, C. Gong, L. Lin, Y. M. Zhu, W. W. Liu, Y. Cheng, S. L. Zhuang, and Z. Z. Xu, ACS. Photonics. **3**, 2338 (2016).

[12] A. T. Schneider, Phys. Rev. A **82**, 033825 (2010).

[13] H. Hirori, A. Doi, F. Blanchard, and K. Tanaka. Appl. Phys. Lett. **98**, 091106 (2011).

[14] G. Y. Tsaur and J. Wang, Phys. Rev. A. **80**, 2554 (2009).

[15] G. R. Plateaua, N. H. Matlis, O. Albert, C. Tóth, C. G. R. Geddes, C. B. Schroeder, J. van Tilborg, E. Esarey, and W. P. Leemans, in *Advanced Accelerator Concepts: Proceedings of the Thirteenth Advanced Accelerator Concepts Workshop*, edited by C. B. Schroeder, W. Leemans, and E. Esarey, AIP Conf. Proc. No. 1086 (AIP, Melville, NY, 2009), pp. 707–712.

[16] S. Antipov, C. Jing, P. Schoessow, A. Kanareykin, V. Yakimenko, A. Zholents, and W. Gai, Rev. Sci. Instrum. **84**, 022706 (2013).

[17] A. Gopal, S. Herzer, A. Schmidt, P. Singh, A. Reinhard, W. Ziegler, D. Brömmel, A. Karmakar, P. Gibbon, U. Dillner, T. May, H-G. Meyer, and G. G. Paulus, Phys. Rev. Lett. **111**, 074802 (2013).

[18] Y. Liu, A. Houard, B. Prade, A. Mysyrowicz, A. Diaw, and V. T. Tikhonchuk, Appl. Phys. Lett. **93**, 051108 (2008).

[19] E. Matsubara, M. Nagai, and M. I. Ashida, J. Opt. Soc. Am. B **30**, 1627 (2013).

[20] N. Karpowicz, X. Lu, and X.-C. Zhang, J. Mod. Opt. **56**, 1137 (2009).

[21] V. Blank, M. D. Thomson, and H. G. Roskos, New J. Phys. **15**, 075023 (2013).

[22] J. Y. Zhao, W. Chu, L. J. Guo, Z. Wang, J. Yang, W. W. Liu, Y. Cheng, and Z. Z. Xu, Sci. Rep. **4**, 3880 (2014).

[23] K. S. Youngworth and T. G. Brown, Opt Express **7**, 77 (2000).

[24] C. D'Amico, A. Houard, S. Akturk, Y. Liu, J. Le Bloas, M. Franco, B. Prade, A. Couairon, V. T. Tikhonchuk, and A. Mysyrowicz, New J. Phys. **10**, 013015 (2008).

[25] A. Houard, Y. Liu, B. Prade, V. T. Tikhonchuk, and A. Mysyrowicz, Phys. Rev. Lett. **100**, 255006 (2008).

[26] F. Jahangiri, M. Hashida, S. Tokita, T. Nagashima, K. Ohtani, M. Hangyo, and S. Sakabe, Appl. Phys. Express. **5**, 026201 (2012).

[27] F. Jahangiri, M. Hashida, S Tokita, T. Nagashima, M. Hangyo, and S. Sakabe, Appl. Phys. Lett. **102**, 191106 (2013).

[28] P. Sprangle, J. R. Penano, B. Hafizi, and C. A. Kapetanakos, Phys. Rev. E **69**, 066415 (2004).

[29] T. Wang, C. Marceau, Y. Chen, Shuai Yuan, F. Théberge, M. Châteauneuf, J. Dubois, and S. L. Chin, Appl. Phys. Lett. **96**, 211113 (2010).

[30] Y. Zhao, W. W. Liu, S. C. Li, D. Lu, Y. Z. Zhang, Y. Peng, Y. M. Zhu, and S. L. Zhuang, Photonics Res. **6**, 296 (2018).

[31] T. Löffler, F. Jacob, and H. G. Roskos, Appl. Phys. Lett. **77**, 453 (2000).

[32] A. Nahata, A. S. Weling, and T. F. Heinz, Appl. Phys. Lett. **69**, 2321 (1996).

[33] Y. Peng, C. Shi, Y. Zhu, M. Gu, and S. Zhuang, PhotoniX **1**, 12 (2020).

[34] Y. Shen, P. C. Upadhya, E. H. Linfield, and A. G. Davies, Appl. Phys. Lett. **82**, 2350 (2003).

[35] Y. Peng, Y. Zhu, M. Gu, and S. Zhuang, Light: Sci. Appl. **8**, 72 (2019).

[36] S. Wang, H. Xiao, and Y. Peng, J. Opt. Soc. Am. B **37**, 3325 (2020).